\



Quality factor enhancement of plasmonic surface latticeresonance by using asymmetric periods

Yunjie Shi(石云杰), Lei Xiong(熊磊), Yuming Dong(董玉明),Degui Sun(孙德贵), and Guangyuan Li(李光元)
Citation: Chin. Phys. B, 2022, 31 (**1**): 014217. DOI: 10.1088/1674-1056/ac1332
Journal homepage: http://cpb.iphy.ac.cn; http://iopscience.iop.org/cpb

What follows is a list of articles you may be interested in

Mode splitting and multiple-wavelength managements of surface plasmon polaritons in coupled cavities

Ping-Bo Fu(符平波) and Yue-Gang Chen(陈跃刚)†
Chin. Phys. B, 2022, 31 (**1**): 014216. DOI: 10.1088/1674-1056/ac0e28

All-fiber laser seeded femtosecond Yb:KGW solid state regenerative amplifier

Renchong Lv(吕仁冲), Hao Teng(滕浩), Jiajun Song(宋贾俊), Renzhu Kang(康仁铸), Jiangfeng Zhu(朱江峰), and Zhiyi Wei(魏志义)
Chin. Phys. B, 2021, 30 (**9**): 094206. DOI: 10.1088/1674-1056/ac11d3

A 37 mJ, 100 Hz, high energy single frequency oscillator

Yu Shen(申玉), Yong Bo(薄勇), Nan Zong(宗楠), Shenjin Zhang(张申金), Qinjun Peng(彭钦军), and Zuyan Xu(许祖彦)
Chin. Phys. B, 2021, 30 (**8**): 084208. DOI: 10.1088/1674-1056/ac0694

Solar energy full-spectrum perfect absorption and efficient photo-thermal generation

Zhefu Liao(廖喆夫), Zhengqi Liu(刘正奇), Qizhao Wu(吴起兆), Xiaoshan Liu(刘晓山), Xuefeng Zhan(詹学峰), Gaorong Zeng(曾高荣), and Guiqiang Liu(刘桂强)
Chin. Phys. B, 2021, 30 (**8**): 084206. DOI: 10.1088/1674-1056/ac0696

Omnidirectional and compact Tamm phonon-polaritons enhanced mid-infrared absorber

Xiaomin Hua(花小敏), Gaige Zheng(郑改革), Fenglin Xian(咸冯林), Dongdong Xu(徐董董), and Shengyao Wang(王升耀)
Chin. Phys. B, 2021, 30 (**8**): 084202. DOI: 10.1088/1674-1056/abe22b

---

Quality factor enhancement of plasmonic surface lattice resonance by using asymmetric periods

Yunjie Shi(石云杰)[1,2], Lei Xiong(熊磊)[2,3], Yuming Dong(董玉明)[2], Degui Sun(孙德贵)[1,†], and Guangyuan Li(李光元)[2,‡]

[1] *Schools of Science, Changchun University of Science and Technology, Changchun* 130022, *China*
[2] *Shenzhen Institute of Advanced Technology, Chinese Academy of Sciences, Shenzhen* 518055, *China*
[3] *School of Information Science and Engineering, Yunnan University, Kunming* 650500, *China*

(Received 18 May 2021; revised manuscript received 4 July 2021; accepted manuscript online 12 July 2021)

We report that using asymmetric lattice periods can enhance the quality factor of plasmonic surface lattice resonances (SLRs) in two-dimensional array of metal-insulator-metal nanopillars in asymmetric dielectric environment. Simulation results show that by adopting appropriate asymmetric lattice periods, the SLR quality factor can be enhanced by 24% compared with the scenario of symmetric periods. We find that the SLR quality factor is optimized when the resonance wavelength is closest to the Rayleigh cutoff wavelength. We also find that the SLRs effect is polarization sensitive in the proposed structure. We expect this work will advance the engineering of SLRs especially in asymmetric dielectric environments, and will promote their applications in sensing.

Keywords: collective resonance, plasmonic nanopillars, surface lattice resonance

PACS: 42.60.Da, 78.67.–n, 78.67.Pt, 73.20.Mf **DOI:** 10.1088/1674-1056/ac1332

1. Introduction

Plasmonic surface lattice resonances (SLRs) supported by metal nanoparticle arrays have been subject to extensive research because of their attractive characteristics such as suppressed radiative loss, narrow linewidth, enhanced fields over large volumes and high quality factors.[1–3] In a diverse range of applications such as ultra-sensitive sensing,[4] tunable and directional nano-lasing,[5,6] and high-performance modulating,[7,8] the high quality factors are vital for the performance.

To date, most literature on SLRs has focused on the symmetric dielectric environment because in this scenario SLRs have high quality factors, which can reach $Q \sim 150$ in the visible regime, an order of magnitude larger than those of localized surface plasmon resonances (LSPRs; $Q \sim 20$).[2] In many applications especially in biochemical sensing, for which the substrate and the superstrate usually have different refractive indices, an asymmetric dielectric environment is desirable. In an asymmetric environment such as air/glass dielectric environment, however, the quality factors of SLRs supported by metal nanorod arrays have been shown to be relatively low, which were shown to be $Q \leq 29$ in the visible regime irrespective of under normal incidence or under oblique incidence, as summarized in our previous work.[9] In order to tackle this challenge, Yang *et al.*[9] proposed a novel type of SLRs supported by a two-dimensional (2D) array of metal-insulator-metal (MIM) nanopillars, the thickness of each layer of MIM, material, scattering unit width, and unit interval were simulated, and found that this SLR prefers the asymmetric dielectric environment: the more asymmetric the dielectric environment, the larger the quality factor. More specifically, in an asymmetric air/glass dielectric environment, the quality factor of SLR can reach $Q = 62$ under normal incidence, which is more than twice of those of conventional SLRs supported by metal nanorods under the same condition. However, there remains much room for improving the quality factor of this novel SLR, which is relatively low compared with SLRs in symmetric dielectric environment.

In order to improve the quality factor of SLRs, diverse approaches have been proposed or demonstrated. Over the years, various illumination conditions, spatial arrangements of nanoparticles, nanoparticle sizes, shapes, materials, dielectric environments, and operation wavelengths have been explored.[1–3,10] For example, Huttunen *et al.*[11] compared in-plane and out-of-plane SLRs in hexagonal and in square lattices, and found that out-of-plane SLRs in hexagonal lattice have larger quality factors than the others because of stronger inter-nanoparticle coupling. Zhou *et al.*[12] proposed a resonant cavity array grating and achieved a quality factor of 580 at the wavelength of 750 nm. Quite recently, Yang *et al.*[13] and Deng *et al.*[14] respectively proposed SLRs supported by arrays of nanohemispheres, and showed that by annealing the metal nanorods into nanohemispheres, the SLR quality factor can be greatly enhanced. However, most of these approaches focused on symmetric lattice periods. Asymmetric lattice periods in x and y directions, that is $\Lambda_y \neq \Lambda_x$, have also shown to

†Corresponding author. E-mail: sundg@cust.edu.cn
‡Corresponding author. E-mail: gy.li@siat.ac.cn

© 2022 Chinese Physical Society and IOP Publishing Ltd

be important for the quality factor of SLRs supported by 2D arrays of metal nanostructures. In 2014, Nikitin[15] fixed the lattice period in y direction and found that the quality factor of SLRs supported by 2D gold nanoparticle arrays can be greatly improved by varying the lattice period in x direction. However, the lattice period in y direction was believed to have negligible effects and thus was excluded from discussion.[15] Chen *et al.*[16] also investigated SLR using the asymmetric lattice periods. However, the effects of the asymmetric lattice periods on the SLR quality factor were not investigated.

In this work, we propose to adopt the asymmetric lattice periods in order to enhance the quality factor of SLRs supported by 2D MIM nanopillar arrays, which prefer asymmetric dielectric environments. Results will show that in asymmetric air/polymer dielectric environment with a refractive index contrast of $1.0/1.52$, the SLR quality factor can be improved from $Q = 62$ to $Q = 77$ by changing the symmetric periods (as adopted in Ref. [9]) into asymmetric periods under normal incidence, corresponding to an enhancement of 24%. The effects of the lattice periods in x and y directions will be systematically investigated.

2. Simulation setup

Figure 1 illustrates the 2D MIM nanopillar array standing on the substrate of refractive index n_{sub} and surrounded by air ($n_0 = 1$). The side length of the square-shaped MIM nanopillar is w, the heights of the top and the bottom gold ridges are h_{tp} and h_{bt}, respectively, and that of the central insulator layer is h_{ct}. The lattice periods in x and y directions are Λ_x and Λ_y, respectively. Plane wave light with unitary electric field intensity ($|E_0|^2 = 1$) impinges onto the structure from air at normal incidence ($\theta = 0$).

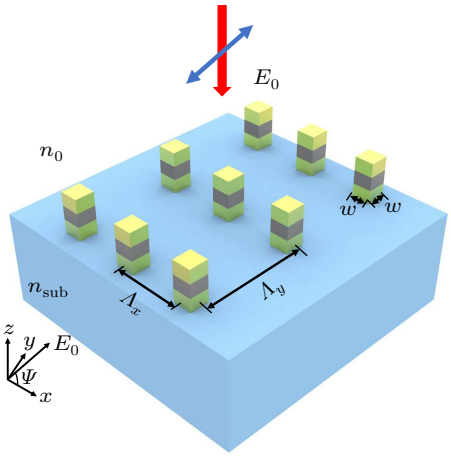


Fig. 1. Schematic of a 2D array of MIM nanopillars with asymmetric lattice periods of Λ_x and Λ_y in asymmetric air/glass dielectric environment. Plane wave light impinges onto the structure under normal incidence with polarization angle Ψ.

The reflectance and transmittance spectra, as well as the near field distributions, are calculated with a home-developed package for fully vectorial rigorous coupled-wave analysis (RCWA). With the calculated reflectance and transmittance spectra R and T, we evaluate the extinction, scattering, and absorption cross section spectra of individual nanoparticles in an array using the following equations:

$$\sigma_{\text{ext}} = (1 - T) \cdot (\Lambda_x \Lambda_y \cos\theta), \tag{1}$$

$$\sigma_{\text{scat}} = R \cdot (\Lambda_x \Lambda_y \cos\theta), \tag{2}$$

$$\sigma_{\text{abs}} = (1 - R - T) \cdot (\Lambda_x \Lambda_y \cos\theta), \tag{3}$$

where θ is the plane wave light incidence angle ($\theta = 0$).

In all the simulations, we take $n_{\text{sub}} = 1.52$ (polymer PU), use silica with $n_{\text{I}} = 1.45$ for the central "I" layer, and adopt gold with wavelength-dependent refractive indices tabulated in Ref. [17]. Unless specified, we consider x polarization (i.e., $\Psi = 0^\circ$) and set $h_{\text{tp}} = h_{\text{bt}} = 140$ nm, $h_{\text{ct}} = 160$ nm, and $w = 180$ nm, which are taken from our previous work using the symmetric periods.[9]

3. Results and discussion

Figure 2 shows the calculated extinction, scattering and absorption cross section spectra of a 2D array of MIM nanopillars with the symmetric lattice periods of $\Lambda_x = \Lambda_y = 450$ nm and a 2D array of MIM nanopillars with the asymmetric lattice periods of $\Lambda_x = 270$ nm and $\Lambda_y = 450$ nm. Results show that for the 2D array of MIM nanopillars with the symmetric lattice periods, there exists a narrow dip locating at 700 nm within the broadband peak in the scattering or the absorption cross section spectrum. Correspondingly, at 700 nm the extinction cross section spectra shows a narrow peak. The 2D array of MIM nanopillars with the asymmetric lattice periods has similar scattering, absorption and extinct cross section spectra as the structure with the symmetric periods. The major difference is that the former has much narrower and slightly blue-shifted scattering and absorption dips (or extinct peak). At the wavelengths of these dips/peaks, as we will show later, SLRs are excited. In terms of the quality factor, which can be calculated by the ratio of the resonance wavelength to the linewidth of the scattering cross section spectra, the 2D array with the symmetric lattice periods has much larger quality factor of $Q = 62$, and the array with the asymmetric periods has the largest quality factor of $Q = 77$. In other words, by changing the symmetric periods into the asymmetric ones, the quality factor can be enhanced by 24%.

In Fig. 3, we plot the simulated near-field electric field distributions at wavelengths of the dips in the scattering cross section spectra for both the symmetric and the asymmetric periods. Figure 3(a) shows that for the 2D array of MIM nanopillars with the symmetric periods, the electric fields are greatly enhanced over a large volume and the enhancement factor

reaches $|E|^2/|E_0|^2 = 300$, featuring the SLR. For the 2D array of MIM nanopillars with the asymmetric periods, figure 3(b) shows that the electric fields outside the MIM nanopillar are also greatly enhanced and the enhancement factor reaches $|E|^2/|E_0|^2 = 160$.

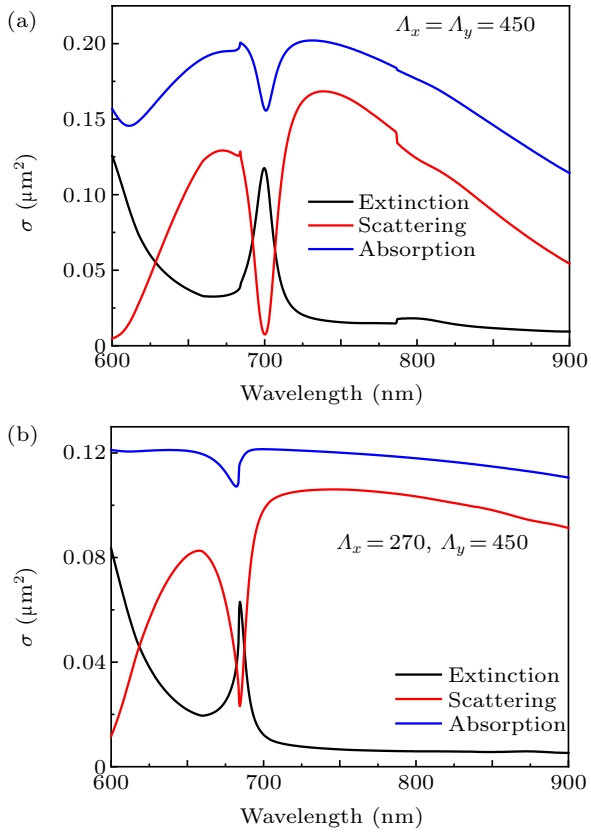


Fig. 2. Extinction (black), scattering (red) and absorption (blue) cross section spectra of 2D array of MIM nanopillars with (a) symmetric lattice periods of $\Lambda_x = \Lambda_y = 450$ nm, and (b) asymmetric periods of $\Lambda_x = 270$ nm and $\Lambda_y = 450$ nm.

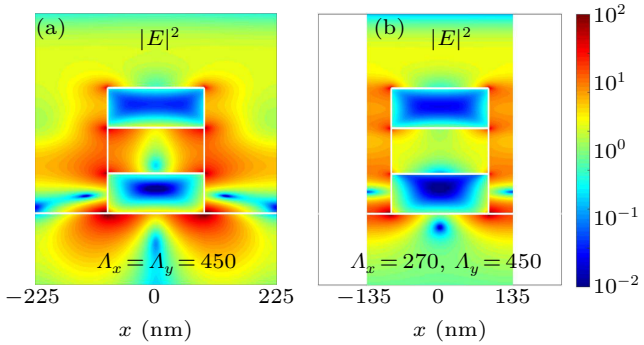


Fig. 3. Simulated electric field distributions of 2D array of MIM nanopillars with (a) symmetric and (b) asymmetric lattice periods at the scattering cross section dips in Fig. 2. The MIM nanopillars are outlined by rectangles, and the air/substrate interface is indicated by the horizontal line.

We now systematically investigate the effects of the periods'asymmetry on the SLR quality factor by varying one lattice period while keeping the other fixed. The reflectance spectra and the corresponding quality factors as functions of the lattice period Λ_x are shown in Fig. 4. The Rayleigh cutoff wavelengths of $(0,\pm1)$ and $(\pm1,0)$ orders are also plotted by the white lines. Here the Rayleigh cutoff wavelength of (m_x, m_y) order is determined by

$$k_0 n_0 = \left|\hat{x}k_0 n_0 \sin\theta + \hat{x}m_x 2\pi/\Lambda_x + \hat{y}m_y 2\pi/\Lambda_y\right|, \qquad (4)$$

where $\theta = 0$ since we restrict ourselves to normal incidence.

We find that as Λ_x increases from 230 nm to 530 nm while Λ_y is fixed to be 450 nm, the reflection dip firstly approaches and then deviates from the horizontal Rayleigh cutoff wavelength line of $(0,\pm1)$ order, and finally intersects with the Rayleigh cutoff wavelength line of $(\pm1,0)$ order. Correspondingly, the SLR quality factor exhibits two peaks of $Q = 77$ and $Q = 69$ when $\Lambda_x = 270$ nm and $\Lambda_x = 470$ nm, which are indicated by the leftmost and the central vertical dashed lines, and for which the reflection dips are closest to the Rayleigh cutoff wavelengths of $(0,\pm1)$ order and $(\pm1,0)$ order, respectively. As Λ_x further increases above 490 nm, indicated by the rightmost vertical dashed line, the quality factor decreases dramatically below 19.

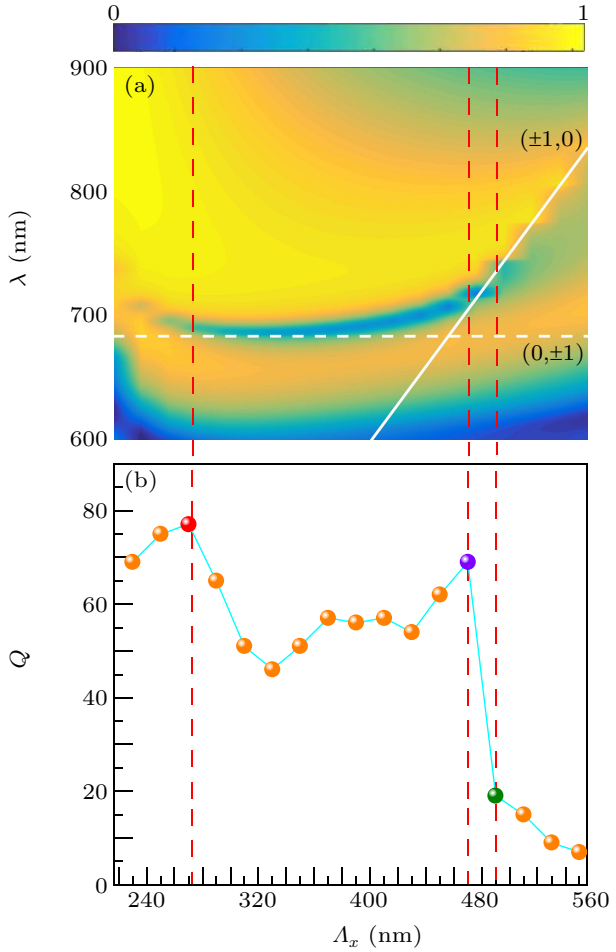


Fig. 4. (a) Reflectance spectra and (b) the corresponding quality factors of the MIM nanopillar array as functions of Λ_x for fixed $\Lambda_y = 450$ nm. The white solid and dashed lines indicate the Rayleigh cutoff wavelengths of $(\pm1,0)$ and $(0,\pm1)$ orders, respectively. The vertical red dashed lines are for $\Lambda_x = 270$ nm, 470 nm, and 490 nm.

On the other hand, if we fix $\Lambda_x = 450$ nm and Λ_y varies between 230 nm and 550 nm, figure 5(a) shows that the wavelengths for the reflection dips firstly keep almost constant

for $\Lambda_y \leq 450$ nm, or have almost constant distance from the Rayleigh cutoff wavelength of the $(\pm1,0)$ order, and then intersect with the Rayleigh cutoff wavelength of the $(0,\pm1)$ order at $\Lambda_y = 470$ nm, as indicated by the vertical dashed line. Correspondingly, figure 5(b) shows that the SLR quality factor firstly keeps almost constant, and then decreases dramatically as Λ_y increases above 470 nm.

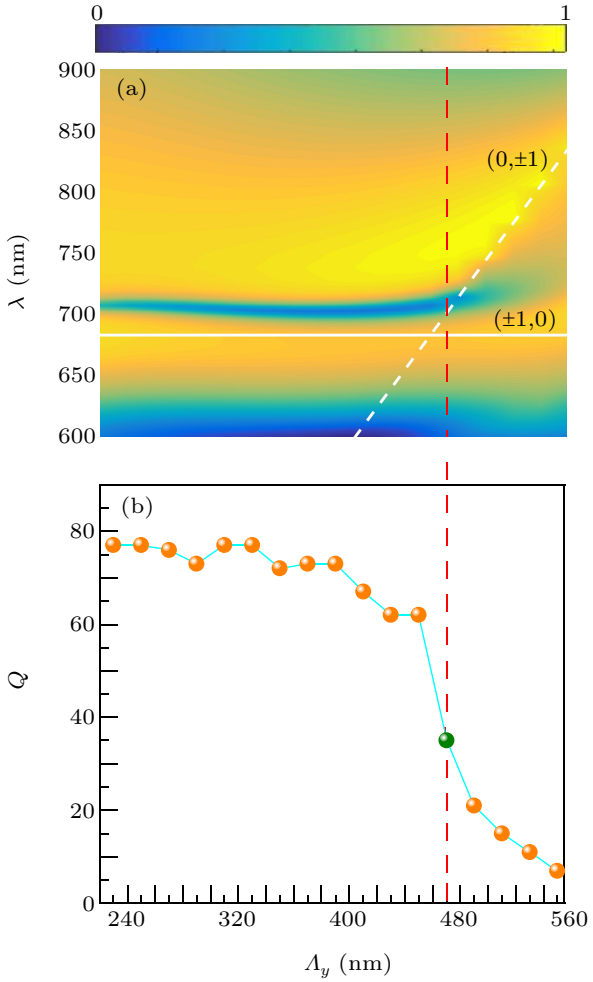


Fig. 5. (a) Reflectance spectra and (b) the corresponding quality factors of the MIM nanopillar array as functions of Λ_y for fixed $\Lambda_x = 450$ nm. The white solid and dashed lines indicate the Rayleigh cutoff wavelengths of $(\pm1,0)$ and $(0,\pm1)$ orders, respectively. The vertical red dashed lines are for $\Lambda_y = 470$ nm.

The distinct responses of reflectance spectra as function of Λ_x and Λ_y in Figs. 4 and 5 are due to the linear polarization of the incidence. This suggests that the SLR in the proposed structure with the asymmetric periods is polarization sensitive. We now verify this statement by comparing the scattering cross section spectra of three different polarizations with $\Psi = 0°$ (the electric field is polarized along the x direction), 90° (the electric field is polarized along the y direction), and 45°. Figure 6(a) shows that for the structure with the symmetric periods of $\Lambda_x = \Lambda_y = 450$ nm, the scattering cross section spectra are exactly the same for the three polarizations. In contrast, for the structure with the asymmetric periods of $\Lambda_x = 270$ nm and $\Lambda_y = 450$ nm, σ_{scat} is polarization sensitive. For $\Psi = 90°$, the dip in the scattering cross section spectra shifts to $\lambda = 698$ nm, consistent with the SLR wavelength for $\Psi = 0°$ with $\Lambda_x = 450$ nm and $\Lambda_y = 270$ nm in Fig. 5(a). For $\Psi = 45°$, there are two dips locating exactly at those for $\Psi = 0°$ and $\Psi = 90°$, since the polarization of $\Psi = 45°$ can be treated as the combination of those of $\Psi = 0°$ and $\Psi = 90°$. Therefore, we expect the scattering cross section spectra for the circular polarizations could also have two dips locating at exactly the same wavelengths for the linear polarization of $\Psi = 45°$, because a circular polarization can also be treated as the combination of those of $\Psi = 0°$ and $\Psi = 90°$ except with a 90° phase difference.

We should note that asymmetric periods do not always come with higher SLR quality factors than symmetric periods. Figure 7 shows that for $h_{\text{tp}} = h_{\text{bt}} = 160$ nm, the SLR supported by the structure with the symmetric periods of $\Lambda_x = \Lambda_y = 450$ nm has higher quality factor of $Q = 50$ than that with the asymmetric periods of $\Lambda_x = 270$ nm and $\Lambda_y = 450$ nm ($Q = 42$), and that for $h_{\text{tp}} = h_{\text{bt}} = 120$ nm, the structure with the symmetric periods supports SLR with $Q = 49$ whereas that with the asymmetric periods does not support SLR within the wavelength range of interest.

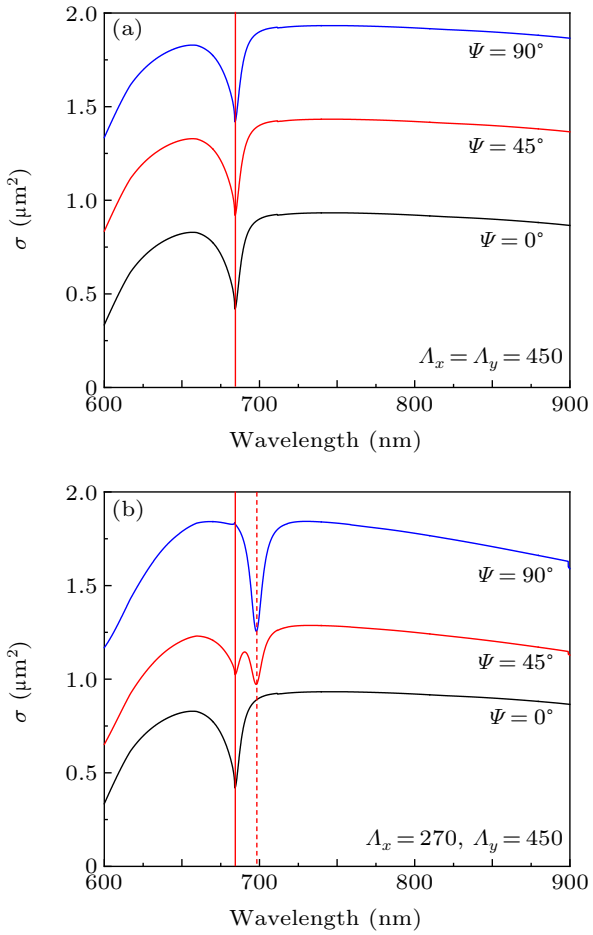


Fig. 6. Scattering cross section spectra of the structure under study with (a) symmetric periods of $\Lambda_x = \Lambda_y = 450$ nm and (b) asymmetric periods of $\Lambda_x = 270$ nm and $\Lambda_y = 450$ nm for polarization angles of $\Psi = 0°$, 45°, and 90°.

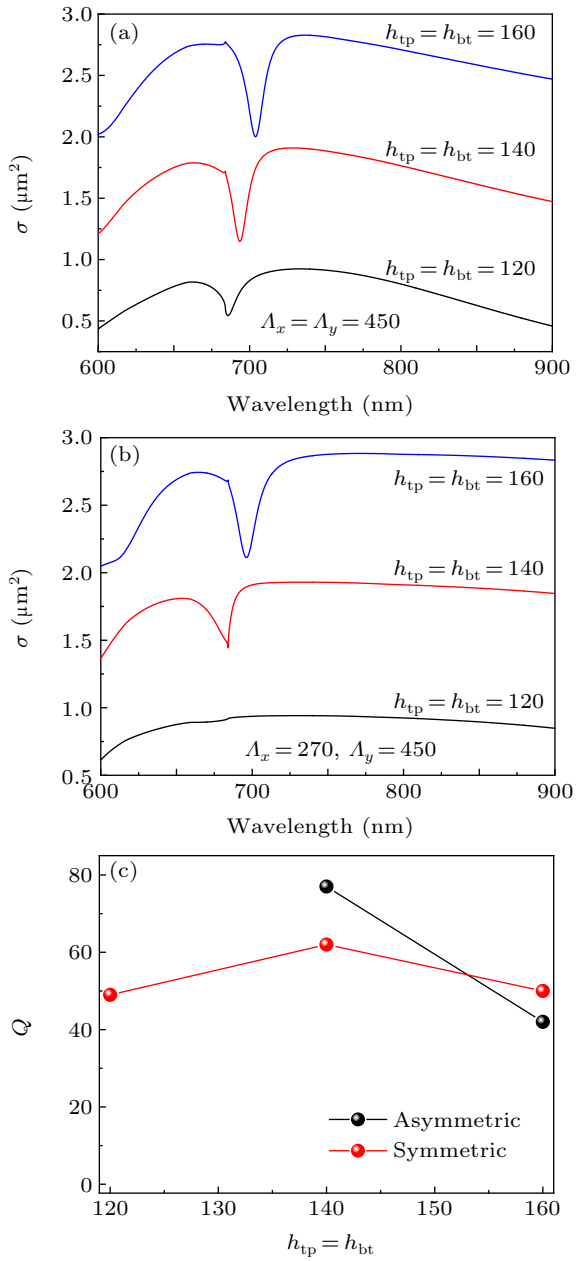


Fig. 7. Scattering cross section spectra of the structure under study with (a) symmetric periods of $\Lambda_x = \Lambda_y = 450$ nm and (b) asymmetric periods of $\Lambda_x = 270$ nm and $\Lambda_y = 450$ nm for different gold thicknesses of $h_{tp} = h_{bt} = 160$ nm, 140 nm, and 120 nm. (c) The corresponding quality factor Q.

4. Conclusion

In conclusion, we have shown that changing the symmetric lattice periods into the asymmetric periods can enhance the quality factor of SLRs supported by MIM nanopillars in asymmetric dielectric environment by 24%, from 62 to 77. Near-field pictures have shown that the SLR quality factor improvement originates from stronger inter-nanopillar coupling. Investigating the effects of asymmetric lattice periods systematically, we have showed that by varying Λ_x while fixing Λ_y, the SLR quality factor exhibits two peaks when the resonance wavelengths are closest to the Rayleigh cutoff wavelengths of the $(0, \pm 1)$ order and the $(\pm 1, 0)$ order, respectively. When Λ_x is fixed, the SLR quality factor almost keeps constant over a large range of Λ_y, from which the resonance wavelength is almost independent. When one of the lattice periods is too large, the SLR quality factor decreases dramatically. We expect Q improvement will advance the engineering of the SLRs supported by the MIM nanopillar array in an asymmetric dielectric environment, and will promote the SLRs' applications especially in sensing.

Acknowledgment

Project supported by the State Key Laboratory of Advanced Optical Communication Systems and Networks, China (Grant No. 2019GZKF2).

References

[1] Wang W, Ramezani M, Vkevinen A I, Trm P, Rivas J G and Odom T W 2017 *Mater. Today* **21** 303
[2] Kravets V G, Kabashin A V, Barnes W L and Grigorenko A N 2018 *Chem. Rev.* **118** 5912
[3] Rajeeva B B, Lin L and Zheng Y 2018 *Nano Res.* **11** 4423
[4] Chen J, Fan W, Zhang T, Tang C, Chen X, Wu J, Li D and Yu Y 2017 *Opt. Express* **25** 3675
[5] Zhou W, Dridi M, Suh J Y, Kim C H, Co D T, Wasielewski M R, Schatz G C and Odom T W 2013 *Nat. Nanotechnol.* **8** 506
[6] Yang A, Hoang T B, Dridi M, Deeb C, Mikkelsen M H, Schatz G C and Odom T W 2015 *Nat. Commun.* **6** 1
[7] Thackray B, Thomas P A, Auton G, Rodriguez F J, Marshall O P, Kravets V G and Grigorenko A N 2015 *Nano Lett.* **15** 3519
[8] Lilley G, Messner M and Unterrainer K 2015 *Opt. Mater. Express* **5** 2112
[9] Yang X, Xiao G, Lu Y and Li G 2019 *Opt. Express* **27** 25384
[10] Liu J Q, He M D, Wang D Y, Tang X M, Zhang X J and Zhu Y Y 2014 *J. Phys. D: Appl. Phys.* **47** 045303
[11] Huttunen M J, Dolgaleva K, Törmä P and Boyd R W 2016 *Opt. Express* **24** 28279
[12] Zhou J, Liu X, Fu G, Liu G, Tang P, Yuan W, Zhan X and Liu Z 2020 *Nanotechnology* **31** 285501
[13] Yang X, Xiong L, Lu Y and Li G 2020 *J. Phys. D* **53** 465109
[14] Deng S, Li R, Park J E, Guan J, Choo P, Hu J, Smeetsd P J M and Odom T W 2020 *Proc. Natl. Acad. Sci. USA* **117** 23380
[15] Nikitin A G 2014 *Appl. Phys. Lett.* **104** 061107
[16] Chen J, Xu R, Mao P, Liu Y, Tang C, Liu J and Zhang L 2014 *Mater. Lett.* **136** 205
[17] Johnson P B and Christy R W 1972 *Phys. Rev. B* **6** 4370